Smart Structures and Systems, *Vol. 15, No. 3 (2015) 627-643*
DOI: http://dx.doi.org/10.12989/sss.2015.15.3.627

Cable with discrete negative stiffness device and viscous damper: passive realization and general characteristics

Lin Chen[1a], Limin Sun[1b] and Satish Nagarajaiah[*2]

[1]*State Key Laboratory for Disaster Reduction of Civil Engineering, Tongji University, Shanghai 200092, P.R. China*
[2]*Department of Civil and Environmental Engineering, and Dept. of Mechanical Engineering, Rice University, Houston, TX 77005, USA*

(Received November 27, 2014, Revised February 8, 2015, Accepted February 15, 2015)

Abstract. Negative stiffness, previously emulated by active or semi-active control for cable vibration mitigation, is realized passively using a self-contained highly compressed spring, the negative stiffness device (NSD).The NSD installed in parallel with a viscous damper (VD) in the vicinity of cable anchorage, enables increment of damper deformation during cable vibrations and hence increases the attainable cable damping. Considering the small cable displacement at the damper location, even with the weakening device, the force provided by the NSD-VD assembly is approximately linear. Complex frequency analysis has thus been conducted to evaluate the damping effect of the assembly on the cable; the displacement-dependent negative stiffness is further accounted by numerical analysis, validating the accuracy of the linear approximation for practical ranges of cable and NSD configurations. The NSD is confirmed to be a practical and cost-effective solution to improve the modal damping of a cable provided by an external damper, especially for super-long cables where the damper location is particularly limited. Moreover, mathematically, a linear negative stiffness and viscous damping assembly has proven capability to represent active or semi-active control for simplified cable vibration analysis as reported in the literature, while in these studies only the assembly located near cable anchorage has been addressed. It is of considerable interest to understand the general characteristics of a cable with the assembly relieving the location restriction, since it is quite practical to have an active controller installed at arbitrary location along the cable span such as by hanging an active tuned mass damper. In this paper the cable frequency variations and damping evolutions with respect to the arbitrary assembly location are then evaluated and compared to those of a taut cable with a viscous damper at arbitrary location, and novel frequency shifts are observed. The characterized complex frequencies presented in this paper can be used for preliminary damping effect evaluation of an adaptive passive or semi-active or active device for cable vibration control.

Keywords: stay cable; vibration control; negative stiffness device; viscous damping; frequency loci

1. Introduction

Cable damped by a local damper, since first considered in 1980s (Kovacs 1982), has received

∗Corresponding author, Professor, E-mail: Satish.Nagarajaiah@rice.edu
[a] Ph.D. Candidate, E-mail: l.chen.tj@gmail.com
[b] Professor, E-mail: lmsun@tongji.edu.cn

http://www.techno-press.org/?journal=sss&subpage=8 ISSN: 1738-1584 (Print), 1738-1991 (Online)

considerable attention subsequently, because cable/damper systems are of both theoretical interest and practical significance. In the context of structural control (Spencer and Nagarajaiah 2003), cables are crucial structural components of cable-stayed bridges, but susceptible to problematic vibrations (Hikami and Shiraishi 1988), posing interesting control problems which can be solved analytically due to the homogeneous cable properties and extended to other more complex or discrete systems with local control units (Main and Krenk 2005, Krenk and Høgsberg 2014). Besides, most of cable vibrations of concern can be suppressed by the attached damper, and associated implementations are worldwide (Chen *et al*. 2003, Fujino *et al*. 2012).

The basic problem of a cable/damper system is the achieved cable damping when a linear viscous damper (VD) is attached near cable support, which has been fully solved (Pacheco *et al*. 1993, Krenk 2000, Tabatabai and Mehrabi 2000, Main and Jones 2002a). Further, to simulate real cable/damper systems, other parameters pertaining to the cable have been included, such as cable bending stiffness (Hoang and Fujino 2007, Main and Jones 2007a, b), cable sag (Xu *et al*. 1998, Krenk and Nielsen 2002) and inclination (Xu and Yu 1998); dampers apart from the linear viscous type have also been addressed, such as by taking damper intrinsic stiffness (Zhou *et al*. 2014a), nonlinearity (Main and Jones 2002b, Hoang and Fujino 2009), and damper support flexibility (Sun and Huang 2008, Huang and Jones 2011) into account. Especially, three key parameters, namely cable sag, flexibility and damper support stiffness, have been treated together to formulate general formulas for practical damper design (Fujino and Hoang 2008). In addition, research interest has also extended to a cable with a damper at arbitrary location (Main and Jones 2002a, Main and Jones 2007a, Sun and Chen 2015) or with two dampers (Caracoglia and Jones 2007a, Hoang and Fujino 2008), and hybrid cable networks with both cross-ties and dampers (Caracoglia and Jones 2007b, Zhou *et al*. 2014b).

The aforementioned studies indicate that positive stiffness introduced at the damper location (due to the damper intrinsic stiffness) decreases the relative damper deformation during cable vibrations, and hence impairs the damping effect that can be attained. The negative stiffness realized by active control or equivalently by semi-active control, conversely, enables the increment of the displacement of the cable at the damper location and hence improves the damper performance. Similar findings were presented in Krenk and Høgsberg (2005) where a damper with fractional damping was considered with parameters corresponding to negative stiffness, which indicated that the damper would provide a phase lead instead of phase lag damping force (Høgsberg and Krenk 2006); the added mass due to the damper installation was also found to have an weakening effect, thus increasing the damping effect.

Negative stiffness characteristics were originally observed from the hysteretic loops produced by friction, semi-active or active algorithm for structural protection (Iemura *et al.*2003, 2006), referred to as apparent negative stiffness or pseudo-negative-stiffness (PNS). The important role of PNS played in semi-active and active strategies has been subsequently recognized, and the idea of PNS has therefore been widely resorted to for optimal controller design, associated studies including Iemura*et al*.(2009), Li *et al*. (2008), Ou and Li (2010), Høgsberg (2011), Weber and Boston (2011) and to name a few. Notwithstanding, it is until only recently that true passive negative stiffness (not pseudo-negative stiffness achieved through active or semi-active means) has been achieved by adaptive passive negative stiffness device (NSD) (Sarlis *et al*. 2013, Pasala *et al*. 2013, 2014). The NSD devices have been theoretically and experimentally evaluated for their effectiveness and advantages, when combined with viscous dampers (VD), for seismic protection.

In this study, the passive NSD is applied for the first time to weaken a cable at the damper location and thus improve the damping effect, as a cost-effective alternative of semi-active or active

cable control (Johnson *et al*. 2003, 2007). Besides, noteworthy is that the linear NSD-VD assembly, or a so-called pseudo-viscoelastic (PVE) damper (Li *et al*. 2008) can replace an active or semi-active device for dynamic analysis based on the equivalence of control force-deformation curves corresponding, respectively, to the (semi-) active device and the PVE damper. This simple strategy has adequate accuracy while avoiding the time-consuming numerical integration which is required to solve the responses of a cable equipped semi-active or active devices, such as magneto-rheological (MR) damper or active tuned mass damper (Johnson *et al*. 2003, 2007, Huang *et al*. 2012). However, only the case when the PVE damper located near cable support has been treated in the aforementioned studies. It is also important to evaluate the effect of arbitrary location of such (semi-) active and passive devices along the cable, for example, by hanging a smart tuned mass damper (Nagarajaiah 2009, Weber *et al*. 2011, Sun *et al*. 2014, Sun and Nagarajaiah 2014).Thus the understanding of a taut cable with a NSD-VD assembly at arbitrary location is of theoretical interest, since it can in turn guide the design of an adaptive passive or semi-active or active control device for cable vibration mitigation.

This paper first presents the passive realization of the negative stiffness device at the damper location of a cable, and then deals with the nonlinear behavior of the NSD. The general dynamic characteristics are subsequently discussed for the taut cable with a linear NSD-VD assembly at arbitrary location.

2. Passive negative stiffness device for cable vibration control

2.1 Negative sitffness device

Passively, negative stiffness can be realized in the lateral direction of a pre-compressed spring, and magnification mechanism can be added accordingly (Sarlis *et al*. 2013) in practice. The pre-compressed spring is directly used here without magnification, while associated results can be extended to the case when magnification mechanism is added. The NSD is arranged in parallel with a viscous damper, resulting an assembly illustrated in Fig. 1, where, k_s is the stiffness of the pre-compressed spring; l is the compressed spring length and c_d is the damper coefficient. The force provided by the assembly is

$$F_d(u) = -c_d\dot{u} + k_s\left[\Delta - \left(\sqrt{l^2+u^2} - l\right)\right]\frac{u}{\sqrt{l^2+u^2}} \tag{1}$$

where $u(t)$ is cable displacement at the damper and Δ is the spring initial deformation.

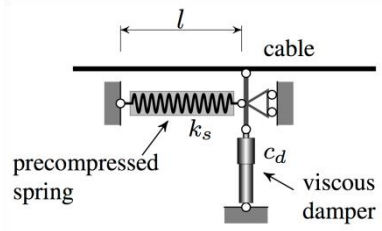

Fig. 1 Schematic of the NSD-VD assembly for cable vibration control

It is worth noting that since the external passive damper is usually installed near one cable anchorage, the displacement at the damper is quite small during cable vibrations, less than 10 mm typically. Considering the length of a compressed spring of l= 1 m, apparently $u<<l$, the negative stiffness is almost a constant and then the force is approximated as

$$F_d(u) \approx -c_d\dot{u} - ku, \quad k = -k_s \frac{\Delta}{l} \tag{2}$$

where k is the approximate negative stiffness coefficient.

2.2 Cable attached with NSD-VD assembly

A taut cable with a NSD-VD assembly is illustrated in Fig. 2, where, m = cable mass per unit, c = cable intrinsic damping, T = cable tension, L = cable length, and x_d denotes the damper location. The cable is still modeled as a taut string owing to practical considerations: cable inclination or sag of practical range for most stay cables has been found insignificant for cable dynamics (Irvine 1981, Tabatabai and Mehrabi 2000); and the bending stiffness of a cable is generally small and difficult to be precisely measured in practice.

2.2.1 Linear approximation

Complex modal analysis (Krenk 2000) can be conducted to appreciate the cable damping due to a linear damper in parallel with a linear spring regardless of the positive or negative spring constant. By defining the following non-dimensional parameters

$$\bar{k} = \frac{kx_d}{T}, \bar{c}_d = \frac{c_d}{\sqrt{Tm}} \tag{3}$$

the maximal modal damping can be then expressed (Krenk and Høgsberg 2005, Li *et al*. 2008) as

$$\zeta_{i,\text{opt}} \approx \frac{1}{1+\bar{k}} \cdot \frac{x_d}{2L} \tag{4}$$

and the corresponding optimal non-dimensional damper coefficient is approximated by

$$\bar{c}_{d,\text{opt}} \approx \left(1+\bar{k}\right) \cdot \frac{1}{i\pi\, x_d / L} \tag{5}$$

Further, following the "universal form" (Krenk and Høgsberg 2005), the additional damping due to an arbitrary damper for mode i is expressed as

$$\zeta_i \approx \frac{x_d/L}{1+\bar{k}} \cdot \frac{\bar{c}_d/\bar{c}_{d,\text{opt}}}{1+\left(\bar{c}_d/\bar{c}_{d,\text{opt}}\right)^2} \tag{6}$$

The preceding equations suggest that when $\bar{k} < 0$ (the system stability requires that $\bar{k} > -1$, Li *et al*. 2008) the additional damping is increased and correspondingly the optimal damper coefficient is decreased for each cable mode, which can be clearly seen from Fig. 3.

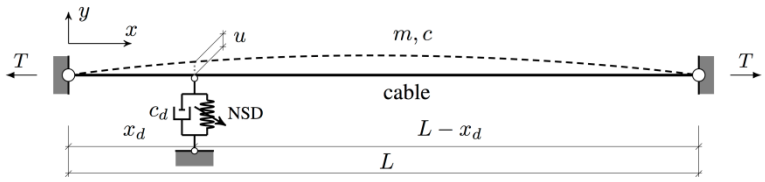

Fig. 2 A taut cable with a NSD-VD assembly

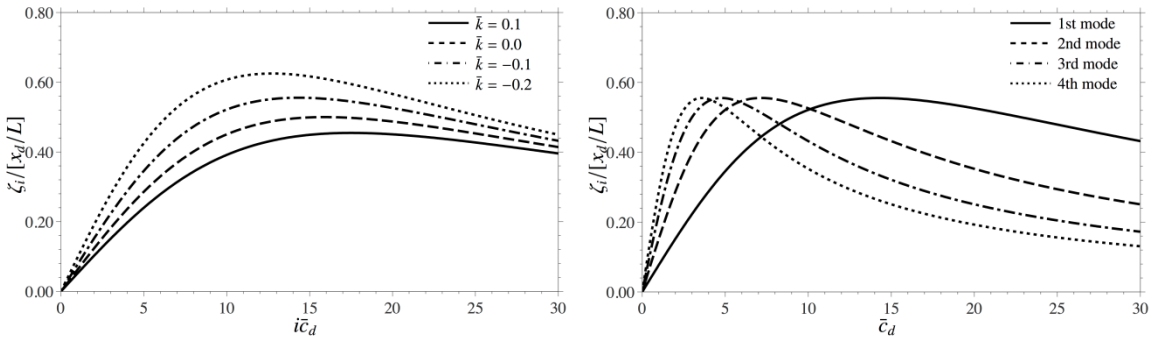

(a) for varied $\bar{k}$ (b) for varied modes when $\bar{k}$ =-0.1

Fig. 3 Damping curves of a cable with a NSD-VD assembly at $\bar{x}_d$ =0.02

2.2.2 Effect of displacement-dependent negative stiffness

Cable discretized by modal decomposition

Taking the nonlinear force generated by the assembly into account, the continuous cable has to be decomposed in modal coordinate for numerical analysis (Pacheco *et al*. 1993, Johnson *et al*. 2007, Li *et al*. 2008). Motions of the cable/damper system are governed by the following non-dimensional equation

$$\ddot{\bar{y}}\left(\bar{x},\bar{t}\right)+\bar{c}\cdot\dot{\bar{y}}\left(\bar{x},\bar{t}\right)-\frac{1}{\pi^2}\bar{y}''\left(\bar{x},\bar{t}\right)=\bar{f}\left(\bar{x},\bar{t}\right)+\bar{F}_d\bar{\delta}\left(\bar{x},\bar{x}_d\right) \tag{7}$$

where those non-dimensional properties, shown with hats, are related to the cable parameters by

$$\bar{t}=\omega_0 t,\bar{x}=\frac{x}{L},\bar{c}=\frac{c}{m\omega_0},\bar{y}\left(\bar{x},\bar{t}\right)=\frac{y\left(x,t\right)}{L},\omega_0=\frac{\pi}{L}\sqrt{\frac{T}{m}} \tag{8}$$

in which ω_0 is the fundamental natural frequency of a taut cable. The excitation force and the damping force are also normalized as

$$\bar{\delta}\left(\bar{x}-\bar{x}_d\right)=L\delta\left(\bar{x}-\bar{x}_d\right),\ \bar{f}\left(\bar{x},\bar{t}\right)=\frac{Lf\left(x,t\right)}{\pi^2 T},\ \bar{F}_d\left(\bar{u}\right)=\frac{F_d\left(u\right)}{\pi^2 T} \tag{9}$$

Substitution of Eqs. (1) and (3) into Eq. (9) leads to

$$\bar{F}_d\left(\bar{u}\right)=-\frac{\bar{c}_d}{\pi}\dot{\bar{u}}-\frac{\bar{k}}{\pi^2\bar{x}_d}\left[\frac{1}{\sqrt{1+\left(\bar{u}/\bar{l}\right)^2}}\left(1+\frac{1}{\bar{\Delta}}\right)-\frac{1}{\bar{\Delta}}\right]\bar{u} \tag{10}$$

with the normalized initial spring deformation $\bar{\Delta}=\Delta/l$ and compressed spring length $\bar{l}=l/L$.

In order to solve Eq. (7), cable transverse deflection is usually approximated using a finite series as $\bar{y}(\bar{x},\bar{t})=\sum_{i=1}^{N}q_i(\bar{t})\phi_i(\bar{x})$, where $q_i(\bar{t})$ is generalized displacement and $\phi_i(\bar{x})$ is the shape function. The subscript *i* indicates the mode number and *N* denotes the total number of cable modes retained. The continuous system is thereby discretized to

$$\mathbf{M}\ddot{\mathbf{q}}+\mathbf{C}\dot{\mathbf{q}}+\mathbf{K}\mathbf{q}=\bar{\mathbf{f}}+\left[\phi_i\left(\bar{x}_d\right)\right]\cdot\bar{F}_d \tag{11}$$

where $q = [q_1\, q_2\, q_3\, \ldots q_N]^{\mathrm{T}}$ and the superscript $^{\mathrm{T}}$ indicates a transpose operation. The mass, damping and stiffness matrices depend on the set of shape functions used: sine series, corresponding to mode shapes of a taut string, were traditionally used (Pacheco *et al*. 1993); Johnson *et al*. (2007) further introduced the static deflection shape of a string with a concentrated force at the damper location in addition to the sine series, to reduce the number of modes needed for numerical convergence; besides, Main (2002) found that two typical mode shapes, namely the undamped mode shape and the mode shape corresponding to the cable clamped at the damper location, are sufficient to capture near resonant responses of that mode. Here, the widely validated shape functions proposed by Johnson *et al*. (2007) are used and the static deflection shape function is designated as mode 1. The mass and stiffness matrices, $\mathbf{M} = [\,m_{i_1 i_2}\,]$ and $\mathbf{K} = [\,k_{i_1 i_2}\,]$, are given as

$$m_{i_1 i_2}=\begin{cases}\dfrac{1}{3} & i_1=i_2=1\\ \delta_{i_1 i_2}/2 & i_1>1, i_2>1,\\ \dfrac{\sin\left(i_m\pi\bar{x}_d\right)}{\bar{x}_d\left(1-\bar{x}_d\right)i_m^2\pi^2} & \text{otherwise}\end{cases}\qquad k_{i_1 i_2}=\begin{cases}\dfrac{1}{\bar{x}_d\left(1-\bar{x}_d\right)\pi^2} & i_1=i_2=1\\ \left(i_1-1\right)^2\delta_{i_1 i_2}/2 & i_1>1, i_2>1\\ \dfrac{\sin\left(i_m\pi\bar{x}_d\right)}{\bar{x}_d\left(1-\bar{x}_d\right)\pi^2} & \text{otherwise}\end{cases} \tag{12}$$

where i_1 and i_2 are mode indices, and $i_m = \max(i_1,i_2)-1$. The damping matrix is $\mathbf{C}=\bar{c}\mathbf{M}$.

Numerical results

Given cable parameters, external excitations and the control force at damper location, cable responses can be obtained by integrating Eq. (11). It is important to point out that the nonlinearity considered here is light ($u<<l$) and local ($x_d<<L$) so that cable free decay can still be used to capture the additional damping due to the external damping device.

With the focus on cable resonant vibrations, the excitation force is expressed as

$$\bar{f}\left(\bar{x},\bar{t}\right)=p\sin\left(i_p\bar{t}\right)\phi_{i_p+1}\left(\bar{x}\right) \tag{13}$$

$$\bar{\mathbf{f}}=p\sin\left(i_p\bar{t}\right)\left[\phi_p\right] \tag{14}$$

where $\phi_p(1)=\sin(i_p\pi\bar{x}_d)/[\bar{x}_d(1-\bar{x}_d)i_p^2\pi^2]$, $\phi_p(i_p+1)=1/2$ and $\phi_p(i)=0$ otherwise. Index i_p denotes the mode to be excited and *p* represent the amplitude of the excitation.

Since the damper location is much more limited for long cables where NSDs are needed, $\bar{x}_d$ = 0.02 is adopted here for exemplification. A NSD of $\bar{k}$ = -0.33 is attached to increase the attainable damping by 50 percent over that provided by a viscous damper according to Eq. (4), and the corresponding optimum damper coefficient for the first mode is computed from Eq. (5). On the configuration of the NSD, it is considered that $\bar{\Delta}$ = 0.5, namely the pre-compression is half of the compressed spring length, and $\bar{l}$ =0.005 (e.g., *l*=1 m for a cable of *L*=200 m). The resonant responses for the first mode were numerically integrated for the cable with the NSD in parallel with an optimum damper under the excitation $p=1\times10^{-4}$, where N=20 modes were retained (Johnson *et al*. 2007). The cable was excited for 53 periods to reach the stationary vibration and then allowed to freely decay. The response at the mid-span is illustrated in Fig. 4(a), and corresponding damping ratio is computed from the peaks of the free decay response as illustrated in Fig. 4(b), ζ_1=0.0153, which is a bit larger than 0.015 obtained from Eq. (4). Fig. 4(b) also shows that the damping ratio is almost displacement-independent in this case.

As demonstrated by the control force versus the cable velocity at the damper in Fig. 5(b), the assembly is able to provide both dissipative and non-dissipative forces at the damper location, which is advantageous to semi-active control where only dissipative force is generated (Johnson *et al*. 2007). Since the nonlinear force is generated merely by the NSD, the force due to the negative stiffness introduced to the cable, as the second term in Eq. (1) or Eq. (10), denoted as $\bar{F}_{\mathrm{ns}}$, is plotted in Fig. 5(a) with respect to the damper deformation, and the total control force is also showed. It is clearly shown that in this case the negative stiffness is almost constant, because $\bar{u}$ is below 3×10^{-4} that is far less than $\bar{l}$ =0.005.

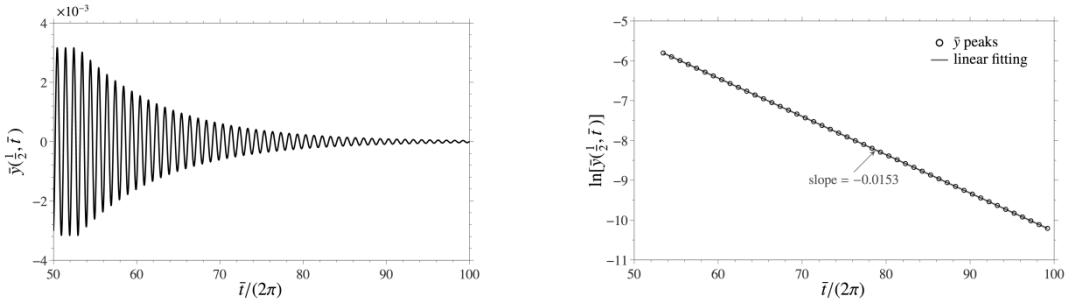

(a) free decay at the mid-span (b) peaks of free decay and corresponding fitted line

Fig. 4 Resonant response of a cable with a NSD and an optimum damper, the first mode case

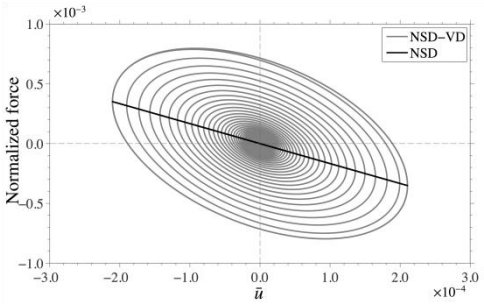

(a) force versus cable displacement at the damper (b) force versus cable velocity at the damper

Fig. 5 Characteristics of the NSD-VD assembly during the cable free decay, the first mode case

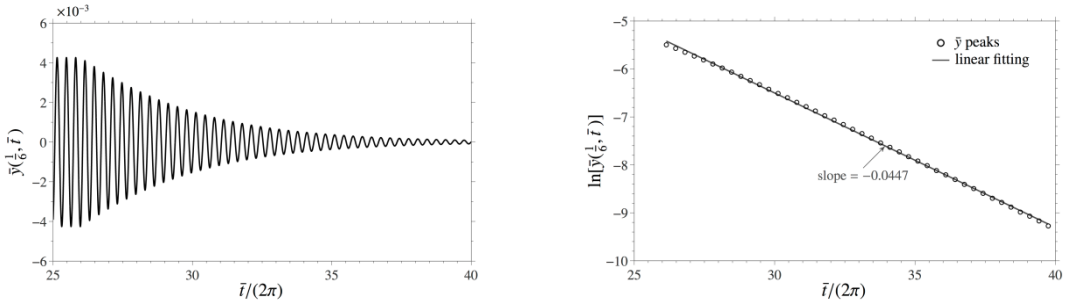

(a) free decay at the 1/6span (b) peaks of free decay and corresponding fitted line

Fig. 6 Resonant response for the third mode case of a cable with a NSD and an optimum damper

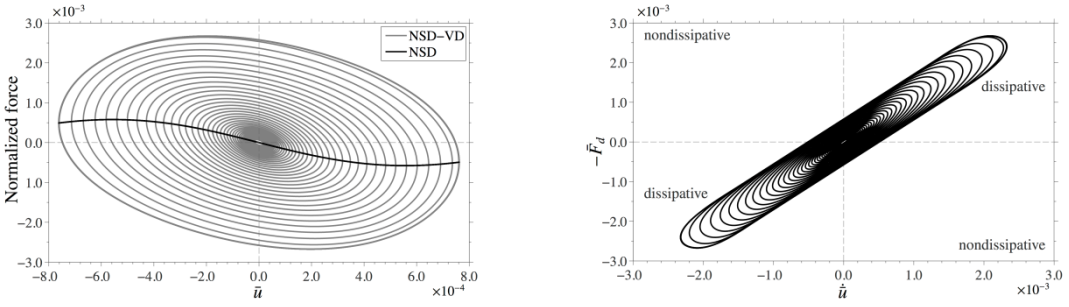

(a) force versus cable displacement at the damper (b) force versus cable velocity at the damper

Fig. 7 Characteristics of the NSD-VD assembly during cable free decay, the third mode case

As also indicated in Eq. (10), the nonlinear force generated by the assembly depends mainly on the ratio $\bar{u}/\bar{l}$. With a reduced $\bar{l}=1\times10^{-3}$l (for instance, *l*=0.5 m for a cable of *L*=500 m) and increasing the excitation amplitude to $p=1\times10^{-3}$ to increase $\bar{u}$ correspondingly, the resulting system was excited during $\bar{t}\in[0,52\pi]$ and then allowed to freely decay. The third mode (i_p=3) free decay is illustrated in Fig. 6(a) and the corresponding modal damping calculation is demonstrated in Fig. 6(b). The additional damping shows visible dependence on the vibration amplitude at the damper compared to the previous case, however, the dependence is still negligible

and the damping can be reliably estimated by the linear fitting as $0.0447/i_p$=0.0149, pretty close to the asymptotic solution from Eq. (4). In this case, the displacement-dependent force due to the NSD is shown in Fig. 7(b) along with the total control force, and the control force versus cable velocity at the damper location is plotted in Fig. 7(b). It is because the damper deformation is comparable to $\bar{l}$.

The passive NSD enables the increment of the displacement of the cable due to negative stiffness at the damper location and hence improves the damper performance. Clearly the larger damping and energy dissipation is evident in Figs. 7(a) and 7(b). It is important to note that even though the negative stiffness is largely dependent on the damper deformation, the linear approximation is still sufficiently accurate for evaluating the additional cable damping. In other words, it can be concluded that for a practical configuration of the NSD for a cable at the damper location, the negative stiffness provided can be safely considered constant, and Eqs. (4)-(6) can be used for the optimum design of the NSD-VD assembly.

2.3 Case study

Based on the approved linear approximation, the relationship between parameters of the NSD with expected stiffness and the cable is obtained by substituting Eq. (3) into Eq. (2)

$$k_s \frac{\Delta}{l} = -\bar{k} \frac{T}{x_d} \tag{15}$$

In the following, a real cable tested by Chen and Sun (2014), with parameters listed in Table 1, is considered to demonstrate the NSD for practical application. The inherent damping ratio of the cable is quite low, ranging from 0.01 to 0.07 of a percent within the vibration amplitudes in the test. To suppress the possible wind/rain-induced variation, it is required that $m\zeta/(\rho D^2) > 10$ (Kumarasena *et al*. 2007) where ρ is the air density (about 1.225 kg/m^3) and D is the cable diameter, that is ζ > 0.43% in this case. Besides, the efficiency factor of a passive device in real-world cable applications can vary from 0.30 to 0.74 (Sun *et al*. 2004). So, the damping ratio of this cable, added by a passive device, is theoretically expected to be larger than 1.17% (considering the mean cable intrinsic damping, 0.04%, and an overall reduction factor of 1/3). When installed at 3.4 m from the cable end, a viscous damper cannot fulfill the requirement, because the maximal damping attainable is 1.01%. A NSD is therefore required with $\bar{k}$ = -0.14 according to Eq. (4), and hence the geometry and stiffness of the pre-compressed spring in Fig. 1is constrained by $k_s \Delta/l$ =157.54 kN/m. This means if a spring with compressed length of 1 meter is chosen, the initial compression force is 157.54 kN, which is feasible from an engineering point of view. Future study is needed to deal with the detailed design of the NSD and the possible magnification mechanism to achieve such a pre-compression force.

Table 1 Parameters of the considered cable

Length L(m)	Mass m(kg/m)	Tension T(kN)	Diameter D(m)	Inherent Damping Ratio (%)	Damper Location x_d(m)
168.25	44.067	3826	0.125	0.01--0.07	3.4

3. General characteristics of a cable with linear NSD-VD at arbitrary location

This section focuses on the general characteristics of a taut cable with a linear NSD-VD assembly at arbitrary location. Hereafter, x_j represents the coordinate originating from each cable end and pointing to the cable center; y_j denotes the transverse displacement of each segment; subscript j is to index the two cable segment divided by the damper; all other parameters are the same as illustrated in Fig. 2.

3.1 Characteristic equation

The characteristic equation of a taut cable with a viscous damper having interior stiffness has been formulated in previous studies, with cable internal damping c=0, as

$$\coth\left[\sqrt{\frac{m}{T}}\lambda x_d\right]+\coth\left[\sqrt{\frac{m}{T}}\lambda\left(L-x_d\right)\right]+\frac{k/\lambda+c_d}{\sqrt{mT}}=0 \tag{16}$$

where λ is the eigen-frequency of the cable/damper system. The above equation is directly used here while the restriction that k>0 (Krenk and Høgsberg 2005, Zhou *et al*. 2014a) or x_d<<L (Li *et al*. 2008) is relieved, and attention is paid to the case where k< 0 and larger frequency shifts are induced, with comparison to the positive and zero stiffness cases.

Introducing the following non-dimensional quantities

$$\mu_1=\frac{x_d}{L},\mu_2=\frac{L-x_d}{L},\tilde{k}=\frac{k\omega_0^{-1}}{\sqrt{mT}},\tilde{\lambda}=\frac{\lambda}{\omega_0} \tag{17}$$

the characteristic equation can then be rewritten in a non-dimensional form

$$\coth\left(\pi\mu_1\tilde{\lambda}\right)+\coth\left(\pi\mu_2\tilde{\lambda}\right)+\tilde{k}/\tilde{\lambda}+\bar{c}_d=0 \tag{18}$$

It is noted that $\bar{k}=\mu_1\pi\tilde{k}$. Correspondingly, the normalized frequency-dependent mode shapes $Y_j(x_j)$ are expressed as

$$Y_j\left(x_j\right)=\gamma\frac{\sinh\left(\pi\tilde{\lambda}\,x_j/L\right)}{\sinh\left(\pi\tilde{\lambda}\mu_j\right)} \tag{19}$$

where γ is the amplitude of $u(t)$.

The complex eigen-frequency can be separated into the real and imaginary parts as

$$\tilde{\lambda}_i=\omega_i\left(\cos\theta_i+\mathrm{i}\sin\theta_i\right)=\sigma_i+\mathrm{i}\varphi_i=-\zeta_i\omega_i+\mathrm{i}\varphi_i \tag{20}$$

where i the square root of -1, and ω_i and θ_i are modulus and phase angle of the complex eigen-frequency; and σ_i and φ_i refer to the real and imaginary parts respectively; the damping ratio and damped frequency then are obtained by $\zeta_i=-\cos\theta_i$ and $\varphi_i=\omega_i\sin\theta_i$.

The system characteristic equation is then separated into the real and imaginary parts as

$$\sum_{j=1,2}\frac{\sinh\left(2\pi\mu_j\omega\cos\theta\right)}{\cosh\left(2\pi\mu_j\omega\cos\theta\right)-\cos\left(2\pi\mu_j\omega\sin\theta\right)}+\frac{\tilde{k}\cos\theta}{\omega}=-\overline{c}_d \tag{21}$$

$$\sum_{j=1,2}\frac{\sin\left(2\pi\mu_j\omega\sin\theta\right)}{\cosh\left(2\pi\mu_j\omega\cos\theta\right)-\cos\left(2\pi\mu_j\omega\sin\theta\right)}+\frac{\tilde{k}\sin\theta}{\omega}=0 \tag{22}$$

where the subscript *i* indicating mode number is omitted for conciseness. Given certain $\tilde{k}$ and μ_1, possible eigen-frequencies can be determined from Eq. (22); the corresponding $\overline{c}_d$ is determined from Eq. (21); and the mode shape is determined afterwards from Eq. (19). Complex $\tilde{\lambda}_i$ of interest is that with positive imaginary part and negative real part, i.e. $\omega_i \geq 0$ and $\pi/2 \leq \theta_i \leq \pi$, corresponding to positive frequency and negative damping.

3.2 Special solutions

Special solutions of the concerned system are first discussed for further characterizing the system in general.

3.2.1 Nonoscillatory decay

For nonoscillatory decay of the system, $\varphi = 0$, and Eq. (22) is thus trivially satisfied regardless of *k*. Also, with purely real eigen-frequencies, Eq. (21) is reduced to

$$\frac{\sinh\left(-2\pi\sigma\mu_1\right)}{\cosh\left(-2\pi\sigma\mu_1\right)-1}+\frac{\sinh\left(-2\pi\sigma\mu_2\right)}{\cosh\left(-2\pi\sigma\mu_2\right)-1}+\frac{\tilde{k}}{-\sigma}=\overline{c}_d \tag{23}$$

Noting the third term approaches to zero and each of the first two terms approaches to unity with $\sigma \to -\infty$, the critical value for the existence of roots of the preceding equation is still $\overline{c}_d$ =2, the same as the case discussed in Main and Jones (2002a).

3.2.2 Nondecaying oscillation

The system oscillates without decaying with purely imaginary eigen-frequencies, e.g., $\tilde{\lambda}_i = \mathrm{i}\varphi_i$. This happens when $\overline{c}_d$ =0, substituting which into the characteristic equation leads to

$$\sin\left(\pi\varphi_i\right)=\frac{\tilde{k}}{\varphi_i}\sin\left(\pi\varphi_i\mu_1\right)\sin\left(\pi\varphi_i\mu_2\right) \tag{24}$$

Solutions to the above equation are denoted as φ_{oi}. Obviously: k= 0, $\varphi_{oi} = i$; when k>0, $\varphi_{oi} \geq i$; for k<0, $\varphi_{oi} \leq i$. The equality for the later two cases is fulfilled when $\sin(\pi\varphi_i\mu_1)\sin(\pi\varphi_i\mu_2)=0$, corresponding to the case when the damper is located at the node of the cable mode *i*.

Similarly, with $\bar{c}_d \to \infty$, the eigen-frequency is also purely imaginary. The characteristic equation is rewritten as

$$\sinh\left(\pi\tilde{\lambda}\right)+\left(\frac{\tilde{k}}{\tilde{\lambda}}+\bar{c}_d\right)\sinh\left(\pi\tilde{\lambda}\mu_1\right)\sinh\left(\pi\tilde{\lambda}\mu_2\right)=0 \tag{25}$$

With bounded $\tilde{k}$ and $\tilde{\lambda}$, solutions for the above equation are cable clamped frequency $\varphi_{ci}^{(j)}=i/\mu_j$, respectively corresponding to the dominant vibration modes of the cable segment *j*.

3.2.3 Critical damping

Oscillatory vibrations approach to critical damping with $\zeta \to 1$ and correspondingly $\sigma \to -\infty$. To discuss the critical damping, the phase equation is rewritten in the form that

$$\sum_{j=1,2}\sin\left(2\pi\varphi\mu_j\right)\cosh\left(2\pi\sigma\mu_{3-j}\right)-\sin\left(2\pi\varphi\right)+\frac{\tilde{k}\varphi}{\omega^2}\prod_{j=1,2}\left[\cosh\left(2\pi\sigma\mu_j\right)-\cos\left(2\pi\varphi\mu_j\right)\right]=0 \tag{26}$$

For bounded φ, when $\sigma \to -\infty$, the above equation is satisfied with $\sin(2\pi\mu_1\varphi)=0$ for $\tilde{k}$ =0 (Main and Jones 2002a), or $\tilde{k}\neq 0$ but $\varphi=0$. In other words, for a damper with positive or negative stiffness, the critical damping cannot be approached for oscillatory vibrations.

3.3 Frequency loci with varied damper location

Complex frequencies have been characterized for a taut cable/damper system (Main and Jones 2002a, Sun and Chen 2015), and the frequency loci with the damper coefficient increasing from zero to infinity have been classified into three distinguished regimes with respect to damper location. The frequency loci of mode *i* originate from the undamped frequency of that mode, while terminate at the frequency corresponding to varied mode with dominant vibration of either cable segment in each regime. In the following, these regimes are extended to a cable with a NSD-VD assembly, where *n* is introduced to denote the node of one mode shape of cable free vibration with *n*=0 referring to the cable end.

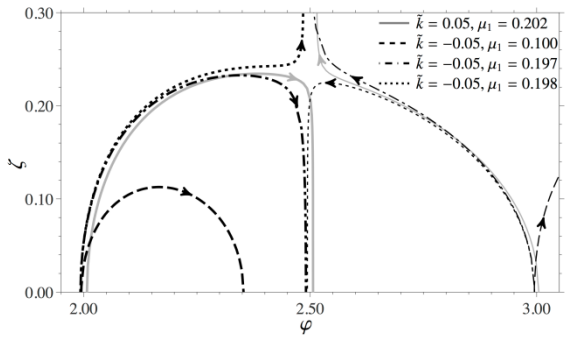

Fig. 8 Frequency loci in regime 1 for mode 2 with varied $\tilde{k}$ and μ_1

3.3.1 Regime 1

In this regime, regardless of the additional stiffness at the damper location, the frequency loci of mode *i* start from the undamped frequency φ_{oi} and terminate at the locked frequency of the longer segment $\varphi_{c(i-n)}^{(2)}$, as illustrated in Fig. 8 for the second mode. However, the upper bound of this regime, which can be analytically expressed only for the zero stiffness case, depends on the stiffness; for positive stiffness, the upper bound is increased while with the negative stiffness, it is decreased. For instance, the upper bound for this regime corresponding to $\tilde{k}$ = 0 is μ_1 =0.2 (Main and Jones 2002a); with a positive stiffness $\tilde{k}$ =0.05, the frequency loci variation is still in this regime for μ_1 =0.202; with a negative stiffness k =-0.05, the frequency loci evolution has already jumped to regime 2 for μ_1 =0.198.

3.3.2 Regime 2

In this regime, variations are observed for the frequency loci evolution of systems where different stiffness is added to the damper, as illustrated in Fig. 9. In particular, when $\tilde{k}$ = 0 (Main and Jones 2002a), the frequency loci in the regime are divided into two distinct branches: one originates from the undamped cable vibration φ_{oi} and terminates at the corresponding critically damped frequency of the longer segment with damping ratio $\zeta \to 1$, and meanwhile $\overline{c}_d$ is increased from zero to 2; the other branch originates from the critically damped frequency of the shorter segment with damping ratio $\zeta \to 1$ and terminates at the fully locked vibration of the short segment, with $\overline{c}_d$ increasing from 2 to infinity. When $\tilde{k}$ > 0, theoretical damping can no longer be approached, as abovementioned, the frequency branch of each mode in this regime originates from the undamped cable vibration φ_{oi} and bends forward to terminate at the clamped vibration of the short cable segment $\varphi_{c(n+1)}^{(1)}$ (Sun and Chen 2015), when the damper is located between the n^{th} node and the $(n+1)^{\text{th}}$ node of the free vibration shape of mode *i*, as illustrated in Figs. 9(a) and 9(b) as a reference.

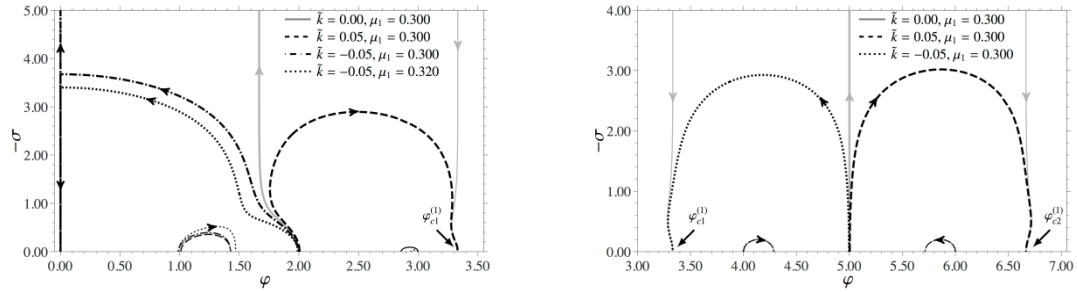

(a) frequency loci of mode 2 with the assembly located between cable end and the first node

(b) frequency loci of mode 5 with the assembly located between the first and second node

Fig. 9 Frequency variation in regime 2 for varied $\tilde{k}$ and μ_1

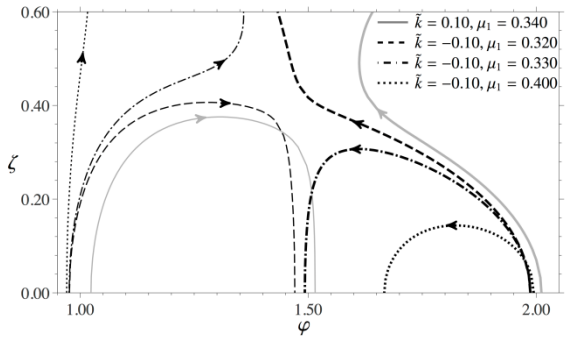

Fig. 10 Frequency loci in regime 3 for mode 2 with varied $\tilde{k}$ and μ_1

With $\tilde{k}$ <0, two sub-cases need to be discussed separately: (1) if the damper is located between the cable support and the first node, the frequency loci starting from φ_{oi} bend leftward to intersect the imaginary axis, as illustrated in Fig. 9(a), and correspondingly terminate at $\varphi = 0$; (2) when the damper is located between the n^{th} node and the $(n+1)^{\text{th}}$ node with $n> 0$, the frequency loci bend also backward but terminate at the clamped vibration frequency of the short cable segment $\varphi_{cn}^{(1)}$, as illustrated in Fig. 9(b) for the fifth mode with the damper near the second anti-node. It is interesting to note that these characteristics of the frequency loci are found to be similar as those for a tensioned beam with a viscous damper presented in Main and Jones (2007a).

3.3.3 Regime 3

Frequency branch of mode *i* categorized in regime 3 originates from the undamped vibration frequency φ_{oi} and terminates at the vibration of the longer segment $\varphi_{c(i-n-1)}^{(2)}$. Nevertheless, the lower bound of this regime depends on $\tilde{k}$: the negative stiffness tends to decrease the lower bound and conversely the positive stiffness increase the lower bound, as illustrated in Fig. 10. As above-illustrated, in each regime varied optimum principle applies for the NSD-VD assembly design, which needs to be solved numerically. Besides, the mode shapes in each regime are not presented for the sake of conciseness, and the readers are advised to refer to Main and Jones (2002a, 2007a) and Sun and Chen (2015).

4. Conclusions

Vibrations of a cable with a NSD-VD assembly were investigated for both practical and theoretical purposes. Typically positive stiffness introduced at the damper location (due to the damper intrinsic stiffness) decreases the relative damper deformation during cable vibrations, and hence impairs the damping effect that can be attained. The passive NSD enables the increment of the displacement of the cable due to negative stiffness at the damper location and hence improves the damper performance. A practical NSD was first implemented to produce true negative

stiffness without any energy input, combined with a VD for cable vibration control. Specifically, asymptotic solutions for the cable with a NSD-VD near cable support have been presented and the nonlinear behavior of the NSD has also been evaluated and confirmed to be negligible for practical configurations of the system. Subsequently, general characteristics of a taut cable with the linear NSD-VD assembly at arbitrary location were discussed in the context of semi-active and active cable vibration control. Varied frequency evolutions of the system have been identified with reference to those of the cable with only the viscous damper, which are extensions of the three regimes of frequency loci for taut cable/damper systems. These complex frequency characteristics can be preliminarily used to evaluate the damping effect of an adaptive passive or semi-active or active device for cable vibration control once the NSD-VD (or PVE damper) assembly of equivalence is determined.

Acknowledgments

The scholarship under the State Scholarship Fund granted by the China Scholarship Council (CSC, File no. 201206260012) for supporting the first author's work at Rice University is gratefully acknowledged.

References

Caracoglia, L. and Jones, N.P. (2007a), "Damping of taut-cable systems: Two dampers on a single stay", *J. Eng. Mech. - ASCE*, **133**(10), 1050-1060.

Caracoglia, L. and Jones, N.P. (2007b), "Passive hybrid technique for the vibration mitigation of systems of interconnected stays", *J. Sound Vib.*, **307**(3-5), 849-864.

Chen, L. and Sun, L. (2014), "Laboratory-scale experimental setup for studying cable dampers", *J. Eng. Mech. - ASCE*, 10.1061/(ASCE)EM.1943-7889.0000878, 04014159.

Chen, Z.Q., Wang, X.Y., Ko, J.M., Ni, Y.Q., Spencer Jr., B.F. and Yang, G. (2003), "MR damping system on Dongting Lake cable-stayed bridge", *Proceedings of the SPIE - The Int. Society for Optical Engineering*, 229-235.

Fujino, Y. and Hoang, N. (2008), "Design formulas for damping of a stay cable with a damper", *J. Struct. Eng. - ASCE*, **134**(2), 269-278.

Fujino, Y., Kimura, K. and Tanaka, H., (2012), *Wind Resistant Design of Bridges in Japan*, Springer, Japan.

Hikami, Y. and Shiraishi, N. (1988), "Rain-wind induced vibrations of cables stayed bridges", *J. Wind Eng. Ind. Aerod.*, **29**(13), 409-418.

Hoang, N. and Fujino, Y. (2007), "Analytical study on bending effects in a stay cable with a damper", *J. Eng. Mech. - ASCE*, **133**(11), 1241-1246.

Hoang, N. and Fujino, Y. (2008), "Combined damping effect of two dampers on a stay cable", *J. Bridge Eng.*, **13**(3), 299-303.

Hoang, N. and Fujino, Y. (2009), "Multi-mode control performance of nonlinear dampers in stay cable vibrations", *Struct. Control Health Monit.*, **16**(7-8), 860-868.

Høgsberg, J.R. and Krenk, S. (2006), "Linear control strategies for damping of flexible structures", *J. Sound Vib.*, **293**(1-2), 59-77.

Høgsberg, J. (2011), "The role of negative stiffness in semi-active control of magneto-rheological dampers", *Struct. Control Health Monit.*, **18**(3), 289-304.

Huang, H., Sun, L. and Jiang, X. (2012), "Vibration mitigation of stay cable using optimally tuned MR damper", *Smart Struct. Syst.*, **9**(1), 35-53.

Huang, Z. and Jones, N.P. (2011), "Damping of taut-cable systems: Effects of linear elastic spring support", *J. Eng. Mech. - ASCE*, **137**(7), 512-518.
Iemura, H. and Pradono, M.H. (2003), "Application of pseudo-negative stiffness control to the benchmark cable-stayed bridge", *J. Struct. Control*, **10**(3-4), 187-203.
Iemura, H., Igarashi, A., Pradono, M.H. and Kalantari A. (2006), "Negative stiffness friction damping for seismically isolated structures", *Struct. Control Health Monit.*, **13**(2-3), 775-791.
Iemura, H. and Pradono, M.H. (2009), "Advances in the development of pseudo-negative-stiffness dampers for seismic response control", *Struct. Control Health Monit.*, **16**(7-8), 784-799.
Irvine, H.M. (1981), *Cable Structures*, Cambridge, MA, U.S.A., MIT Press.
Johnson, E., Baker, G., Spencer, B. and Fujino, Y. (2007), "Semiactive damping of stay cables", *J. Eng. Mech. - ASCE*, **133**(1), 1-11.
Johnson, E.A., Christenson, R.E. and Spencer Jr., B.F. (2003), "Semiactive damping of cables with sag", *Comput. - Aided Civil Infrastruct. E.*, **18**(2), 132-146.
Kovacs, I. (1982), "Zurfrage der seilschwingungen und der seildampfung", *Bautechnik*, **59**(10), 325-332.
Krenk, S. (2000), "Vibrations of a taut cable with an external damper", *J. Appl. Mech. - T. ASME*, **67**(4), 772-776.
Krenk, S. and Høgsberg, J. (2014), "Tuned mass absorber on a flexible structure", *J. Sound Vib.*, **333**(6), 1577-1595.
Krenk, S. and Høgsberg, J.R. (2005), "Damping of cables by a transverse force", *J. Eng. Mech. - ASCE*, **131**(4), 340-348.
Krenk, S. and Nielsen, S.R.K. (2002), "Vibrations of a shallow cable with a viscous damper", *P. Roy. Soc. Lond., Series A*, **458**(2018), 339-357.
Kumarasena, S., Jones, N.P., Irwin, P. and Taylor P. (2007), *Wind-Induced Vibration of Stay Cables*, Report.
Li, H., Liu, M. and Ou, J. (2008), "Negative stiffness characteristics of active and semi-active control systems for stay cables", *Struct. Control Health Monit.*, **15**(2), 120-142.
Main, J.A. (2002), *Modeling the vibrations of a stay cable with attached damper*, Ph.D. Dissertation, Johns hopkins University, Baltimore, Maryland.
Main, J.A. and Jones, N.P. (2002a), "Free vibrations of taut cable with attached damper. I: Linear viscous damper", *J. Eng. Mech. - ASCE*, **128**(10), 1062-1071.
Main, J.A. and Jones, N.P. (2002b), "Free vibrations of taut cable with attached damper. II: Nonlinear damper", *J. Eng. Mech. - ASCE*, **128**(10), 1072-1081.
Main, J.A. and Jones, N.P. (2007a), "Vibration of tensioned beams with intermediate damper. I: Formulation, influence of damper location", *J. Eng. Mech. - ASCE*, **133**(4), 369-378.
Main, J.A. and Jones, N.P. (2007b), "Vibration of tensioned beams with intermediate damper. II: Damper near a support", *J. Eng. Mech. - ASCE*, **133**(4), 379-388.
Main, J.A. and Krenk, S. (2005), "Efficiency and tuning of viscous dampers on discrete systems", *J. Sound Vib.*, **286**(1-2), 97-122.
Nagarajaiah, S. (2009), "Adaptive passive, semiactive, smart tuned mass dampers: identification and control using empirical mode decomposition, Hilbert transform, and short-term fourier transform", *Struct. Control Health Monit.*, **16**(7-8), 800-841, DOI: 10.1002/stc.349.
Ou, J. and Li, H. (2010), "Analysis of capability for semi-active or passive damping systems to achieve the performance of active control systems", *Struct. Control Health Monit.*, **17**(7), 778-794.
Pacheco, B.M., Fujino, Y. and Sulekh, A. (1993), "Estimation curve for modal damping in stay cables with viscous damper", *J. Struct. Eng. - ASCE*, **119**(6), 1961-1979.
Pasala, D., Sarlis, A., Nagarajaiah, S., Reinhorn, A., Constantinou, M. and Taylor, D. (2013), "Adaptive negative stiffness: New structural modification approach for seismic protection", *J. Struct. Eng. - ASCE*, **139**(7), 1112–1123, DOI: 10.1061/(ASCE)ST.1943-541X.0000615.
Pasala, D., Sarlis, A., Reinhorn, A., Nagarajaiah, S., Constantinou, M. and Taylor, D. (2014), "Simulated bilinear-elastic behavior in a SDOF elastic structure using negative stiffness device: Experimental and analytical study", *J. Struct. Eng. - ASCE*, **140**(2), 04013049.
Sarlis, A., Pasala, D., Constantinou, M., Reinhorn, A., Nagarajaiah, S. and Taylor, D. (2013), "Negative

stiffness device for seismic protection of structures", *J. Struct. Eng. - ASCE*, **139**(7), 1124-1133.
Spencer, B. and Nagarajaiah, S. (2003), "State of the art of structural control", *J. Struct. Eng. - ASCE*, **129** (7), 845-856.
Sun, C. and Nagarajaiah, S. (2014), "Study on semi-active tuned mass damper with variable damping and stiffness under seismic excitations", *Struct. Control Health Monit.*, **21**(6), 890-906.
Sun, C., Nagarajaiah, S. and Dick, A. (2014), "Family of smart tuned mass dampers with variable frequency under harmonic excitations and ground motions: closed-form evaluation", *Smart Struct. Syst.*, **13**(2), 319-341.
Sun, L. and Huang, H. (2008), *Design, implementation and measurement of cable dampers for large cable-stayed bridges*, IABSE Congress Report, **17**(16), 242-243.
Sun, L. and Chen, L. (2015), "Free vibrations of a taut cable with a general viscoelastic damper modeled by fractional derivatives", *J. Sound Vib.*, **335**(2015), 19-33.
Sun, L., Shi, C., Zhou, H. and Cheng, W. (2004), "A full-scale experiment on vibration mitigation of stay cable", *Proceedings of the IABSE Symp. Rep., IABSE Symp., Shanghai 2004: Metropolitan Habitats and Infrastructure*, IABSE, Zurich, Switzerland.
Tabatabai, H. and Mehrabi, A.B. (2000), "Design of mechanical viscous dampers for stay cables", *J. Bridge Eng.*, **5**(2), 114-123.
Weber, F. and Boston, C. (2011), "Clipped viscous damping with negative stiffness for semi-active cable damping", *Smart Mater. Struct.*, **20**(4), 045007.
Weber, F., Boston, C. and Maślanka, M. (2011), "An adaptive tuned mass damper based on the emulation of positive and negative stiffness with an MR damper", *Smart Mater. Struct.*, **20**(1), 015012.
Xu, Y.L. and Yu, Z. (1998), "Vibration of inclined sag cables with oil dampers in cable-stayed bridges", *J. Bridge Eng.*, **3**(4), 194-203.
Xu, Y.L., Yu, Z. and Ko, J.M. (1998), "Forced vibration studies of sagged cables with oil damper using a hybrid method", *Eng. Struct.*, **20**(8), 692-705.
Zhou, H., Sun, L. and Xing, F. (2014a), "Damping of full-scale stay cable with viscous damper: Experiment and analysis", *Adv. Struct. Eng.*, **17**(2), 265-274.
Zhou, H., Sun, L. and Xing, F. (2014b), "Free vibration of taut cable with a damper and a spring", *Struct. Control Health Monit.*, **21**(6), 996-1014.